Journal of
Applied Remote Sensing

How does the global Moderate Resolution Imaging Spectroradiometer (MODIS) Fraction of Photosynthetically Active Radiation (FPAR) product relate to regionally developed land cover and vegetation products in a semi-arid Australian savanna?

Birte Schöttker
Stuart Phinn
Michael Schmidt

SPIE

How does the global Moderate Resolution Imaging Spectroradiometer (MODIS) Fraction of Photosynthetically Active Radiation (FPAR) product relate to regionally developed land cover and vegetation products in a semi-arid Australian savanna?

Birte Schöttker,[a] Stuart Phinn,[a] and Michael Schmidt[b]

[a] The University of Queensland , Centre for Spatial Environmental Research, The School of Geography, Planning and Environmental Management, Brisbane QLD 4072, Australia

b.schoettker@uq.edu.au

[b] Remote Sensing Centre, Department of Environment and Resources Management, 80 Meiers Road, Indooroopilly QLD 4068, Australia

Abstract. Spatio-temporally variable information on total vegetation cover is highly relevant to water quality and land management in river catchments adjacent to the Great Barrier Reef, Australia. A time series of the global Moderate Resolution Imaging Spectroradiometer (MODIS) Fraction of Photosynthetically Active Radiation (FPAR; 2000-2006) and its underlying biome classification (MOD12Q1) were compared to national land cover and regional, remotely sensed products in the dry-tropical Burdekin River. The MOD12Q1 showed reasonable agreement with a classification of major vegetation groups for 94% of the study area. We then compared dry-seasonal, quality controlled MODIS FPAR observations to (i) Landsat-based woody foliage projective cover (wFPC) (2004) and (ii) MODIS bare ground index (BGI) observations (2001-2003). Statistical analysis of the MODIS FPAR revealed a significant sensitivity to Landsat wFPC-based Vegetation Structural Categories (VSC) and VSC-specific temporal variability over the 2004 dry season. The MODIS FPAR relation to 20 coinciding MODIS BGI dry-seasonal observations was significant ($\rho < 0.001$) for homogeneous areas of low wFPC. Our results show that the global MODIS FPAR can be used to identify VSC, represent VSC-specific variability of PAR absorption, and indicate that the amount, structure, and optical properties of green and non-green vegetation components contribute to the MODIS FPAR signal.

Keywords: Moderate Resolution Imaging Spectroradiometer (MODIS), Fraction of Photosynthetically Active Radiation (FPAR), total vegetation cover, foliage projective cover, vegetation structural category, Australia, savanna.

1 INTRODUCTION

Tropical savannas[1] are amongst the most dynamic ecosystems worldwide which exhibit a complex array of eco-physiological processes that are driven by space- and time-dependent climate and ground properties in a strongly seasonal and episodic rainfall regime [1, 2]. Tropical savanna ecosystems have adapted to these environmental conditions with vertically and horizontally heterogeneous vegetation cover, while land management practices strongly affect their resilience to change [3, 4].

Tropical savannas provide 75% of the grazing areas worldwide [1], foster a rich biodiversity, account for 30% of the primary production of all terrestrial vegetation [5], and play a significant role in global carbon sequestration [5]. In Australia, the state of Queensland is to more than 75% used for cattle grazing and covered by wood-, shrub-,

[1] Savanna is defined here as in Grace et al. (2006, p 387), as “any tropical ecosystem containing grasses, including woodland and grassland types”.

Received 9 Feb 2010; accepted 4 Jun 2010; published 23 Jun 2010 [CCC: 19313195/2010/$25.00]

and savanna grassland [6]. With two large catchments draining into the Great Barrier Reef (GBR) lagoon, vegetation and land cover estimates are required for input into erosion, water quality, and pasture production models and are great interest to both, the GBR Water Quality Protection Plan and the State's Leasehold Land Strategy (Delbessy Agreement) [7, 8].

Total Vegetation Cover (TVC) is comprised of photosynthetically active vegetation (PV) and non-photosynthetically active vegetation (NPV), including senescent standing matter, dead litter, stems and bark [9, 10]. Estimates of TVC are a prerequisite for the development of comprehensive earth system models, including net primary production and carbon, eco-hydrology, and energy exchange models, as well as for applications related to natural and cultivated vegetation monitoring and climate change [11, 12]. Repeated, synoptic-scale remote sensing estimates of biophysical properties of the TVC and land cover provide a means for extrapolating ground measurements and informing land managers and conservationists. The growth of remote sensing techniques and products over the last decades has delivered useful information at a variety of spatial and temporal scales [as summarized in 13, 14, and as in 15]. However, challenges in the remote sensing of TVC still lie in its complex spectral reflectance which is strongly co-determined by the structural and optical properties of the pixel and scene components. As the quantity of NPV is non-linearly related to the PV mass in grasslands [16], classical spectral vegetation indices have been of limited use for erosion or biomass modelling in these ecosystems [17, 18]. Tropical savannas pose a particular challenge to remote sensing applications due to abundant NPV material being present at most times of the year in a structurally complex and heterogeneous landscape [19], which influences the biophysical and spectral properties of TVC at canopy and landscape scale [20].

In Australia, extensive remote sensing research over the last decades on TVC mapping and monitoring has been conducted with satellite imagery and field observations [21-23]. Australian vegetation poses specific challenges through its dominantly vertical leaf inclination, sparse foliage, irregular crown shapes and clumping [21, 24]. The Queensland Department of Environment and Resource Management (QDERM) has mapped Foliage Projective Cover (FPC) [25], a metric of woody vegetation cover [26], and bare ground [6] using regression-based methods with medium spatial- coarse temporal resolution Landsat Thematic Mapper (TM) and Enhanced Thematic Mapper (ETM+) imagery. Both products build on SLATS archive of more than 1500 geometrically and radiometrically corrected Landsat TM and ETM+ time images of a time series from 1988 to 2004 covering the state with annual coverage or better [21] and extensive field observations of vegetation parameters. FPC values represent a combination of green herbaceous and woody FPC with an error component. The bare ground product describes the inverse of ground cover. More details on the woody FPC product used in this study can be found in Section 2.2.4 of this paper. At a similar spatial resolution, Gill and Phinn (2008) [22] have shown potential and limitations of using spectral unmixing of ASTER data to separate PV, NPV and bare ground at a regional scale. Attempts to estimate TVC with coarse spatial- but high temporal resolution imagery have focused on the decomposition of evergreen (woody) and seasonally green vegetation cover [27, 28]. Milne et al. [29] developed a MODIS bare ground index (BGI) for tropical savanna grasslands in Queensland using MODIS satellite imagery and QDERM's Landsat bare ground product. Section 2.2.5 of this paper provides further information on the MODIS BGI product. Guerschman et al. [30] recently developed high temporal resolution, estimates of PV, NPV, and bare ground for the Australian tropical savanna zone with hyperspectral and multispectral imagery. However, NPV proportions were underestimated by about 40% to 50% in Queensland's heterogeneous landscapes.

For the detection of NPV plant material in remote sensing applications the shortwave infrared wavelengths have been commonly used [31], although the wavelength of photosynthetically active radiation (PAR) (400-700 nm) has also proven useful [19, 32, 33]. PAR is not always used for photosynthesis ('functional PAR') and a significant component can be absorbed by NPV material in tropical savannas [19]. Asner et al. [13] showed in a combined field measurement and radiative transfer modeling approach the effect of NPV components on PAR absorption was more pronounced in areas with a leaf area index (LAI) of less than 3.0, where standing grass litter canopies absorbed almost as much PAR as green grass canopies. Hence is it problematic to assume little or no contribution from NPV components to absorbed PAR by a canopy or landscape. Increased knowledge and improved radiative transfer modelling (RTM) of PAR absorption at leaf, canopy, pixel, and landscape level in different environments [19, 34, 35] has led to the development of a metric termed the fraction of absorbed photosynthetically active radiation (fAPAR) [36, 37]. The fAPAR is of particular importance, because it provides a direct connection between ecosystem structure and function, including nitrogen use, CO2 assimilation, and water loss [19, 38]. Studies using remotely sensed fAPAR have shown sensitivity to NPV components, structural vegetation groups [39, 40], that fAPAR is advantageous over classical vegetation indices particularly in heterogeneous landscapes [17, 41, 42] and open canopies where understory components can affect landscape and canopy fAPAR substantially [19, 43]. Huete and Jackson (1987) [18] also emphasized that the relationship of fAPAR to the Normalized Difference Vegetation Index (NDVI) is particularly complex and non-linear for these kind of ecosystems (i.e. savannas).

The MODIS Global LAI/FPAR (FPAR is synonymous with fAPAR) product (MOD15A2) is one of two operational products worldwide that provide high temporal resolution information on the Fraction of Photosynthetically Active Radiation (FPAR) absorbed by a canopy. The MODIS FPAR product measures the proportion of available radiation in the photosynthetically active wavelengths (400 to 700 nm) that a canopy absorbs, accounting for additional absorption within the canopy due to the interaction between the ground (soil and/or understory) and the canopy [44]. The freely available product offers 8-day composites in 1 km spatial resolution. Limited validation of the global MODIS FPAR product has been published in recent years for savanna or semi-arid ecosystems [36, 41, 42]. However, the MOD15A2 has undergone substantial evaluation and its major limitations are known [45, 46]. Most publications on the MODIS FPAR product compared it to leaf and canopy RTM, such as Oloffson and Eklundh (2007) [43] who included field data. In comparison with field data, Huemmrich et al. (2005) [41] found that the MODIS FPAR product collection 3 overestimated PAR in dry savanna ecosystems by 10% to 15%. Additional validation studies have been published on the MOD15A2 product with field based measurements [41, 42, 47] and fAPAR derived from other sensors [45, 48, 49], however forested areas were the main ecosystem of these investigations. The only validation of the MOD15A2 product in Australia was conducted by Hill et al. (2006) [24], but was for the LAI and not the FPAR product. The MOD15A2 algorithm underlying land cover classification MOD12Q1 has been identified as a limitation as it uses six standardized biomes that might not represent regional land cover characteristics [24, 45].

The aim of this study is to assess the relationship between the high temporal resolution global MODIS FPAR (MOD15A2, collection: C 4) and regionally developed and validated remotely sensed products of vegetation and land cover in the dry-tropical savannas of Queensland, Australia. This study is divided into two main parts: First, the biome classification MOD12Q1 was compared to a national classification of major floristic and structural vegetation groups for one major river catchment draining into the GBR. This was to evaluate the global MODIS FPAR product's potential usability in this environment. We then conducted a strict quality control of the MODIS FPAR product. Second, descriptive statistics of the MODIS FPAR were compared to two coinciding, regionally developed products: (i) a classification of a 2004 Landsat TM and ETM+ woody foliage projective cover product (wFPC) [25] into Vegetation Structural Categories (VSC); and (ii) a time series of MODIS BGI observations (2001-2003) [29]. Both products were produced by QDERM representing the best regionally calibrated and validated products available and together address different structural and fractional components of the TVC.

2 STUDY AREA AND DATASETS

The region of the Burdekin River Catchment (BRC) covers approximately 140 000 km^2 and is the second largest catchment draining into Great Barrier Reef (GBR) lagoon in the tropical, semi-arid parts of Australia (Fig. 1).

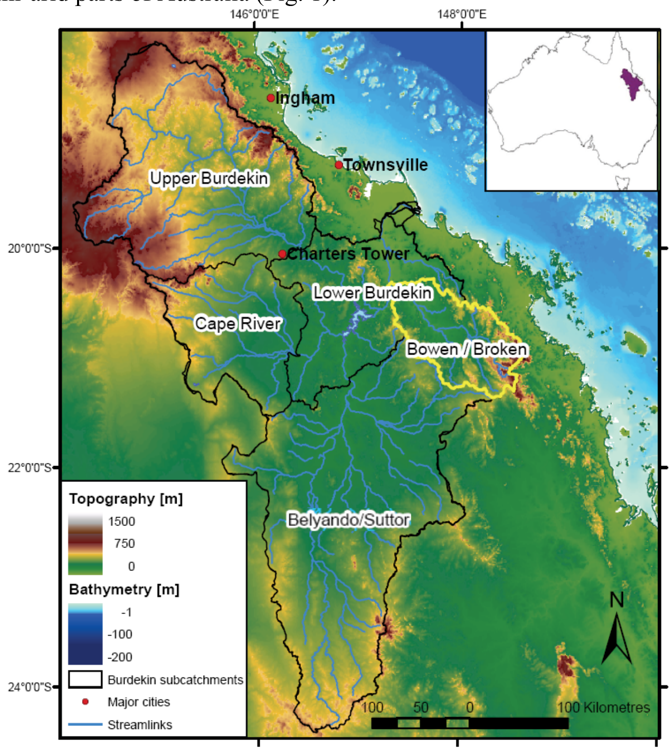

Fig. 1. Topography and bathymetry of the Burdekin River catchment (BRC) region. The outlines of the BRC and its subcatchments are delineated in black line, with the Bowen/Broken River subcatchment (BBRs) emphasized in yellow. Data sources: Geoscience Australia, Hutchinson et al. (2000) [53], and QDERM.

The BRC's climate is characterized by hot wet summers (November to April) and dry, warm winters. For millennia the BRC has experienced water driven erosion, but terrestrial discharge has increased about four fold since European settlement [50]. The focal study site for this research is the Bowen/Broken River subcatchment (BBRs), about 9500 km^2 of the BRC (Fig. 1), was selected as it is representative of the BRC and has been recognized as a 'hot spot' for water driven erosion processes [51, 52]. The annual rainfall in the BBRs 1998-2005 ranged from about 490 mm to 1300 mm with 73% of the average daily rainfall occurring in the wet season. Steeper regions in the east receive more, while 75% of the BBRs in the eastern parts receives less than 800 mm per year [51]. The vegetation in the BBRs is dominated by eucalypt woodland and open woodland, acacia forests, and patches of eucalypt open forests. Most of the western and lower parts of the BBRs are drier and dominated by open woodlands (mainly bloodwoods, Eucalyptus crebra, and Iron or Poplar box) and grasslands [54], rainforest and wet sclerophyll are found in the steeper eastern ranges. The dominant land uses in the BBRs in 2004 were extensive grazing of native and modified pastures (67%) [54] and conservation and natural environments (28%). Land use changes during the period of investigation of this study 2001-2003 have annually accounted for less than 1% of the BBRs catchment area (3.05 km^2 in 2004/2005 and 24.33 km^2 in 2003/2004) based on data from the QDERM Statewide Landcover and Trees Study (SLATS) [25].

2.2 Datasets

2.2.1 Remote Sensing datasets

This study compares remotely sensed total vegetation/land cover products from the Moderate Resolution Imaging Spectroradiometer (MODIS) on board the TERRA (EOS AM-1) spacecraft and the TM and ETM+ instruments onboard the LANDSAT 5 and 7 satellites respectively. The specific global and regionally developed remotely sensed total vegetation/land cover products are listed in Table 1 and are described in more detail below.

Table 1. Overview of remotely sensed total vegetation and land cover products used in this study. Data sources are as indicated: National Aeronautics and Space Administration (NASA) and Land Processes and Distributed Active Archive Centre (LPDAAC); Queensland Department of Environment and Resource Management (QDERM); Commonwealth Scientific and Industrial Research Organisation (CSIRO).

Remotely sensed Product	**Surface parameter measured**	**Spatial resolution**	**Time period selected/ Time steps**	**Data source/ acquisition**
MODIS land cover classification (MOD12Q1, C4, type 3)	Global land cover classification	1 km	2004 annual, 6 biomes	NASA and LPDAAC
MODIS FPAR (TERRA, MOD15A2, C4)	Fraction of Photosynthetically Active Radiation that a plant canopy absorbs **(FPAR)**	1 km	2000-2006 8-day composites	NASA and LPDAAC, CSIRO
LANDSAT 5 TM and 7 ETM+ wFPC	**w**oody **F**oliage **P**rojective **C**over (**wFPC**)	25 m	2004 annual	QDERM
MODIS BGI	**B**are Ground Index (fraction of bare ground)	500 m	2001-2003 16-day composites	QDERM

2.2.2 The MOD12Q1 product

We acquired the MODIS FPAR underlying land cover classification, the global MOD12Q1 annual product in 1 km spatial resolution for 2004 [44]. The MOD12Q1 Type 3 C4 is freely available through the United States Geological Survey's Land Processes and Distributed Active Archive Centre (LPDAAC) data pool (https://lpdaac.usgs.gov/lpdaac/get_data/data_pool). It is an important ancillary data set for the MODIS FPAR algorithm, as it represents the RTM compatible structural land cover classification in six vegetated biomes, derived from supervised decision-tree classification method [55]. Three unvegetated classes are included in the classification for which no FPAR algorithm retrievals are made [55]. Each of the biomes represents a pattern of the architecture of an individual tree (leaf normal orientation, stem-trunk-branch area fractions, leaf and crown size) and the entire canopy (trunk distribution, topography), as well as patterns of spectral reflectance and transmittance of vegetation elements [44]. The soil and/or understory type are also characteristics of the biome, which can vary continuously within given biome-dependent ranges.

2.2.3 The MODIS FPAR product

The global remotely sensed data product we use is a time series of the MODIS FPAR 8-day composites in 1 km spatial resolution from 2000/02 to 2006/12 (MOD15A2, C 4, level 4) [44, 56]. The MOD15A2 is freely available from the LPDAAC [57] and comprises the LAI and the FPAR product and two flag variable files per product [48]. The MODIS FPAR for this study was preprocessed by the Commonwealth Scientific and Industrial Research Organisation (CSIRO) [58] and then provided to the authors. The MODIS FPAR product measures the proportion of available radiation in the photosynthetically active wavelengths (400 to 700 nm; scaled 0 to 1.0) that a canopy absorbs, accounting for additional absorption within the canopy due to the interaction between the ground (soil and/or understory) and the canopy [44]. The MODIS FPAR algorithm is based on a look-up table (LUT) inversion of a model developed from three dimensional radiative transfer (3D-RT) theory. Different model configurations, including spectral and angular signatures of vegetation canopies, are derived based on the MOD12Q1 product [44]. In case the inverse problem cannot be solved, a backup algorithm is triggered which estimates FPAR (and LAI) from their relation to NDVI [56]. Further details on the theoretical algorithm can be found in Knyazikhin et al. (1999) and others [44, 59].

Known limitations of the MODIS FPAR C3 and C4 dataset that influence the accuracy of FPAR retrievals include: (i) uncertainties in input surface reflectances [60]; (ii) uncertainties in the algorithm underlying the global land cover classification MOD12Q1 [24, 45]; and (iii) uncertainties from the model used to build the LUT's [60]. Fensholt et al. (2004) [44] give a comprehensive summary on the research of how these uncertainties influence the LAI and FPAR retrievals. Some uncertainties in the MODIS FPAR product due to (i) and (ii) can be identified and eliminated by using the two MODIS FPAR quality flag variables for quality control of the time-series. The authors are aware of information published in 2008 which refers to the MODIS FPAR C4 product used in this study to be affected by a problem in the code of the C4 MODIS FPAR data since 2004 [61]. C4 data was still provided from LPDAAC until C5 was released in 2008. The problem referred to MODIS FPAR C4 product delivering FPAR estimates under diffuse illumination conditions (standard overcast sky) (pers. comm. Yuri Knyazikhin, 18.11.2008). The deviation is not expected to affect the approach of this study as we conduct comparisons to other remotely sensed data products but not to other FPAR quantities (pers. comm. Yuri Knyazikhin, 18.11.2008).

2.2.4 The LANDSAT wFPC product

The second remotely sensed product used in this study is the Queensland's Landsat TM and ETM+ 2004 woody FPC (wFPC) product [25]. Woody FPC is defined here as the vertically projected percentage cover of photosynthetic foliage from tree and shrub life forms greater than 2 m height" [26], which is the definition adopted by SLATS [25]. The wFPC version used in this study was derived using a time-series of dry season (May-October; 1988-2004) FPC predictions from geometrically and radiometrically corrected TM and ETM+ imagery [26]. The FPC values are assumed to be a combination of green herbaceous and wFPC with an error component. Pixels are classified as non-woody (0% wFPC) or woody (1-100% wFPC) on the basis of thresholds applied to the time-series minimum and normalized standard error of a linear regression line fitted to the FPC series. The wFPC estimates are then generated using a linear robust time-series regression that predicts wFPC for each woody pixel based on the trend across the annual FPC imagery [21]. Validation with estimates of overstory wFPC from airborne Light Detection and Ranging (LiDAR) [21] has shown estimates of woody FPC are predicted from Landsat TM imagery with less than 10% RMSE (pers. comm., John Armston, QDERM).

2.2.5 The MODIS BGI product

A time series of MODIS Bare Ground Index (BGI) product in eight to 16-day composites in 500m spatial resolution from 2001 to 2003 used in this study was developed at the QDERM for monitoring bare ground in tropical savanna grasslands in areas of wFPC of less than 20 to 30% [29, 62]. The MODIS BGI is based on a Landsat TM bare ground product developed by QDERM [6] and was developed for dry seasons over savanna woodlands in the BRC. The MODIS BGI is derived from a time series of combined MODIS Terra and Aqua standardized reflectances to a common solar zenith and azimuth angle using BRDF parameters in combination with semi-empirical models (Ross-thick and Li-Sparse) [62]. The QDERM's Landsat TM bare ground product [6] was used as the response variable in a generalized linear regression analysis to derive the MODIS BGI product [62]. During the analysis, explanatory variates such as MODIS spectral bands, products of bands, logarithms of bands and a full range of BRDF parameters were evaluated [62]. Cross-validation using subsets of the MODIS imagery as training data and calculating prediction root-mean square errors (RMSE) were used to determine the optimal number of terms for the MODIS BGI regression model [62]. Accuracies of the MODIS BGI product in relation to the field observations of bare ground lie around 40% RMSE [29].

2.2.6 Ancillary datasets

A classification of Present Major Vegetation Groups (MVG) was acquired from the Australian National Vegetation Inventory System (NVIS) (updated 2005, version 3.0; NVIS MVG in the following) [63]. The MVG groups reflect the dominant vegetation proportion occurring in a map unit from a mix of several vegetation types based on vegetation floristic (dominant vegetation type, e.g. species) and structural (dominant vegetation form, e.g. cover, growth form and height) data. The NVIS NVG is a compilation of vegetation descriptions and GIS data gathered from over 100 projects by 25 government agencies across all jurisdictions [63]. Input data have different origins and mapping scales as they were sourced from field observations and/or aerial photography and/or remotely sensed imagery [63]. The scale of the input data for the area of the BRC is noted to be 1:100 000 as shown on an online version of the NVIS MVG (http://www.environment.gov.au/about/publications/pubs/poster-major-veg-map.pdf).
The digital NVIS MVG dataset at 100 m spatial resolution is designed for use at a national or state-wide scale, or for simple vegetation descriptions at a regional scale [64], and was used here to evaluate the MOD12Q1. Detailed information on this dataset can be found at the NVIS MVG website (http://www.environment.gov.au/erin/nvis/mvg/index.html#mvg).

Catchment boundaries for this study were derived from a nine second Digital Elevation Model [53].

3 METHODOLOGY

3.1 MOD15A2 underlying land cover classification MOD12Q1

The MOD12Q1 product, the MODIS Land Cover Type 3 classification, which underlies the MODIS FPAR algorithm, was acquired from LPDAAC in 1 km resolution in sinusoidal projection for the year 2004. Two tiles of the MOD12Q1 covering the BRC area were mosaicked and reprojected to the Map Grid of Australia (MGA) 1994, Zone 55 using nearest neighbor resampling. For the comparison of the global MOD12Q1 from 2004 with the national/regional NVIS MVG land cover classification we calculated 'Zonal Tabulate Areas' of the two raster datasets (ArcGIS 9.2). During that process the NVIS MVG land cover classification was resampled to 1 km (nearest neighbor technique). The output table lists the calculated total area of the MOD12Q1 land cover classes that comprise each NVIS MVG land cover class.

3.2 Vegetation Structural Categories

In several previous studies overstory FPC (here wFPC), has been shown to be a more suitable indicator of a plant community's radiation interception and transpiration than the worldwide more commonly used crown cover [26]. Australian plant communities are dominated by trees and shrubs with sparse foliage and irregular crown shapes. Table 2 shows a classification of Australian savannas into VSC representing structural formations as well as floristic associations. The classification in Table 2 includes differing combinations of vegetation over- and understory and proportions of senescent vegetation components based on Fensham (2008) [65]. We classified the regional Landsat wFPC product of the BBRs study site into these VSC by thresholding.

Table 2. Overview of vegetation structural categories (VSC) modified from Fensham (2008) [65] for Australian Savannas. Vertical layering of the vegetation cover is represented through strata, which are split into taller stratum (TS; > 6 m tall) and Lower Stratum (LS; < 6 m tall). LS crown cover increases with decreasing TS cover, which is given in percentage wFPC, grouped into classes 1 to 6.

Crown cover for the LS	**wFPC crown cover equivalent for the TS**	**Vegetation Structural Categories (VSC)**
Crown cover (%)	*Class no. and wFPC range (%)*	
	Class 6 71-100%	Closed Forest
	Class 5 51-70%	Open forest with shrubby understory (not relevant)
	Class 4 31-50%	Open forest with shrubby understory
30-100%	Class 3 11-30%	Woodland with shrubby understory, shrubland
10-30%		Woodland with shrubby understory
0-10%		Woodland
30-100%	Class 2 3-10%	Shrubland
10-30%		Open woodland with shrubby understory
0-10%		Open woodland
30-100%	Class 1 0-2%	Open-scrubs, closed-scrub
10-30%		Open shrubland, shrubland
0-10%		Grassland-herbland

3.3 MODIS FPAR processing

The MOD15A2 C4 product was acquired as HDF-EOS files in unsigned eight bit integer projected onto an Integer Sinusoidal mapping grid [59]. At CSIRO the HDF-EOS gridfiles were collated in an Australian wide mosaic and reprojected to geographic lat/lon projection using the MODIS reprojection Tool (v 3.2a) tool[2] with the nearest neighbor resampling technique to a pixel size of 0.009 degrees at the centre coordinate of the BRC (21°17'37.97''S and 146°45'56.99''E). A time series of the MODIS FPAR from 26/02/2000 to 31/12/2006 was extracted for an area covering the study site of the BRC and reprojected to MGA 1994 Zone 55 using nearest neighbor resampling technique. We further conducted a quality control, excluded fill values, and converted the digital values to their fractional units [59].

[2] http://edcdaac.usgs.gov/landdaac/tools/modis/index.asp

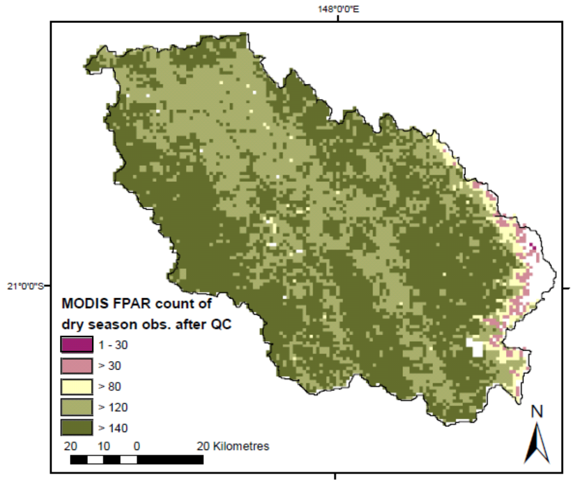

Fig. 2. Count of valid MODIS FPAR pixels per dry season after quality control was applied for the dry season 2004 (n = 157). Blank areas represent no retrievals.

The two flag files of the MOD15A2 were used to exclude FPAR pixels that were not retrieved by the main algorithm (without or with saturation) and/or had 'assumed clear' or contaminated cloud conditions, and that depicted land cover for which the algorithm could not retrieve an estimate [59]. Pixels retrieved by the back-up algorithm were excluded because the algorithm is suggested to fail when pixels are near the soil line and the NDVI is very small, resulting in these pixels being classified as not vegetated [62]. The remaining FPAR retrievals for the time-series after the quality control were counted and are shown per pixel for a selected dry season from May to October in 2004 for the area of the BBRs in Fig. 2. From 157 observations in the 2004 dry season, approximately 80% of the catchment had valuable, quality controlled FPAR retrievals for 75% of the time-series. Largest data gaps of 40 consecutive observations to no retrievals at all occurred in the eastern ranges of dense forests (Fig. 2).

3.4 Comparison of MODIS FPAR to LANDSAT wFPC and MODIS BGI

The MODIS FPAR quality controlled data were used to calculate per-pixel descriptive statistics (mean and standard deviation) for the BBRs study site over the dry season from May to October inclusive 2004. We chose the dry season 2004 because a moderate rainfall event and terrestrial discharge occurred in the following wet season. The comparison of the statistics to the regionally developed products was then structured as follows.

(i) Visual comparison of the Landsat wFPC VSC classes from 2004 (25 m resolution) for the subcatchment of about 9500 km^2 to a false color-composite of MODIS FPAR 2004 dry season descriptive statistics (1 km resolution). An RGB-false color composite consisting of the MODIS FPAR mean in the red band, the standard deviation in the green band, and an empty blue band was used. The Landsat wFPC image from 2004 was classified based on the six VSC classes from Table 2 according to classes of percent wFPC cover.

(ii) Analysis of MODIS FPAR 2004 (1 km resolution) dry season statistics for all VSC classes. A majority filter was applied to the 25 m Landsat wFPC dataset which was resampled then to 1 km (nearest neighbor resampling). We calculated the median, upper and lower quartile per VSC class from the 2004 dry season mean and standard deviation for the BBRs and its surrounding area (17179 km^2). The MODIS FPAR mean values of the VSC classes were arcsine transformed to fulfill the condition of normal distribution for a one-sided ANalysis Of VAriance (ANOVA). For each

VSC class we calculated absolute and relative measures of variability of the MODIS FPAR mean values to provide class specific measures of variability in PAR absorption for that dry season. The coefficient of variation (CV) was used to describe the relative variability within each VSC class.

(iii) Comparison of the time series of MODIS BGI (500 m) for selected homogenous regions <30% wFPC to a time series of 20 dry season coinciding MODIS FPAR observations from 2001 to 2003. The MODIS FPAR product was resampled to 500 m using the nearest neighbor resampling technique. One to three homogeneous regions of 3-10 km^2 were manually selected within the three VSC classes representing < 30% wFPC. Each region was chosen so at least 90% of pixels were of one VSC class, and the regions were evenly distributed over the whole BBRs. MODIS FPAR and BGI values were averaged over these regions per VSC class 1, 2, and 3 (Table 2). No disturbances due to land cover change had been recorded during this period in those regions. The regions of the classes 1 and 2 were aggregated to one class to increase the number of pixels in the homogeneous regions, assuming there would be little difference in FPAR response for such structurally and floristically similar classes.

4 RESULTS

4.1 Comparison of the MOD12Q1 to the NVIS MVG land cover classification

The NVIS MVG and MOD12Q1 classifications for the BRC region are shown in Fig. 3. Visually there appears to be a correspondence between the distribution of "Eucalypt Woodlands" in the MVG classification and "Savanna" in the MOD12Q1 classification. Reasonable agreement in regard to structural characteristics was found between NVIS MVG and MOD12Q1 classifications although the two classifications differ substantially in number of classes (Fig. 3). The global MOD12Q1 divides the globe into six vegetated biomes. The national/regional NVIS MVG classification defines overall 18 major vegetation groups and four non vegetated classes for the BRC region (Fig. 3).

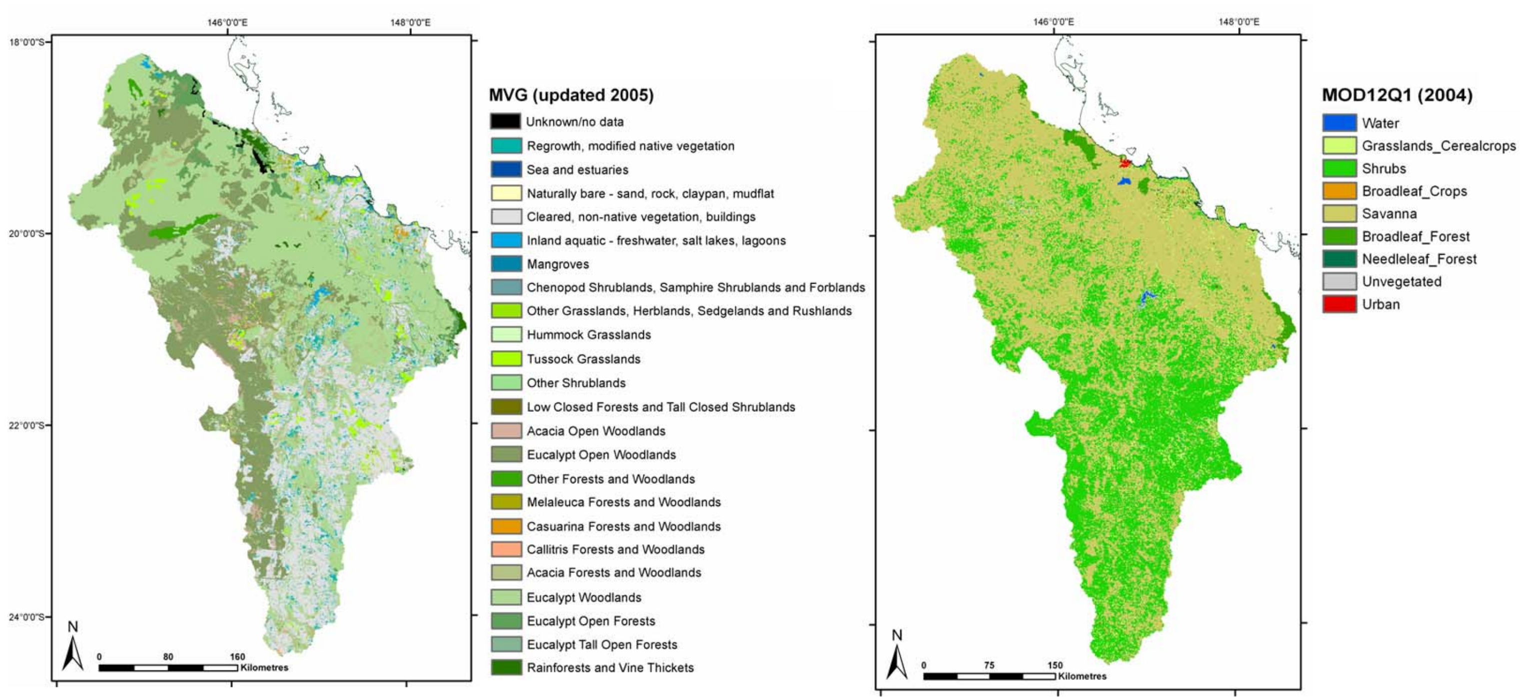

Fig. 3. NVIS MVG land cover classification (left) and MOD12Q1 (right) land cover classification for the BRC region. Date sources: DEWHA [63], Australia [64], and LPDAAC, NASA, US.

A listing of the total areas and percentages of biome classes of the global MOD12Q1 and the national/regional NVIS MVG land cover classes for the BRC region of about 140 000 km^2 are summarized in Table 3. Only the NVIS MVG classes that cover more than 1% of the BRC region are listed. Estimates of the overall area of the study site vary slightly due to resampling of NVIS MVG dataset. The global MOD12Q1 classifies the majority of the study area of the BRC region as "Savanna" or "Shrubs", which together constitute 94.28% of the BRC region. In terms of vegetation structural communities the national/regional NVIS MVG classification shows 77.02% of the BRC region to be entirely wooded, which is less than that shown by the global MOD12Q1 classification (96.82%). However the wooded component of the NVIS MVG class "Cleared, non-native vegetation, buildings" may reduce this difference. The greatest (percentage of area) discrepancy between the two classifications is the 20.88% of the BRC region with the NVIS MVG class "Cleared, non-native vegetation and buildings", which does not have an equivalent class in the MOD12Q1.

Table 3. Total areas and percentages of the global MOD12Q1 type 3 land cover classes (top) and national/regional NVIS MVG land cover classification for the BRC region (bottom) sorted by size of area per class, showing only classes that cover more than 1% of the BRC region.

MOD12Q1		
Land cover class	**Area (km²)**	**Area (%)**
Savanna	81 938	58.39
Shrubs	50 366	35.89
Grassland_Cerealcrops	4 483	3.19
Broadleaf_Forest	2 646	1.89
Unvegetated	538	0.38
Water	195	0.14
Urban	91	0.06
Needleleaf_Forest	48	0.03
Broadleaf_Crops	14	0.01
Sum area	*140 319*	*100.00*

NVIS MVG		
Land cover class	**Area (km²)**	**Area (%)**
Eucalypt Woodlands	56 547	40.30
Eucalypt Open Woodlands	31 343	22.34
Cleared, non-native vegetation, buildings	29 302	20.88
Acacia Forests and Woodlands	6 358	4.53
Eucalypt Open Forests	4 374	3.12
Regrowth, modified native vegetation	3 954	2.82
Tussock Grasslands	1 944	1.39
Acacia Open Woodlands	1 588	1.13
Sum area	*140 313*	*100.00*

Figure 4 shows the percentages of MOD12Q1 classes within all of the NVIS MVG classes and reveals where particular mismatches in both classifications lie. The by area dominant NVIS MVG class of "Eucalypt Woodlands" (Table 3) is dominantly (about 70 %) identified as "Savanna" and to almost one third identified as "Shrubs" by the MOD12Q1 (Fig. 4). The by area second dominant NVIS MVG class "Eucalypt Open Woodlands" (Table 3) is likewise dominantly identified as "Savanna" (to about 60 %) and to about one third identified as "Shrubs" by the MOD12Q1. The NVIS MVG class "Cleared, non-native vegetation and buildings" is not similarly accounted for in the MOD12Q1 and to about 60% represented by the MOD12Q1 class of "Shrubs".

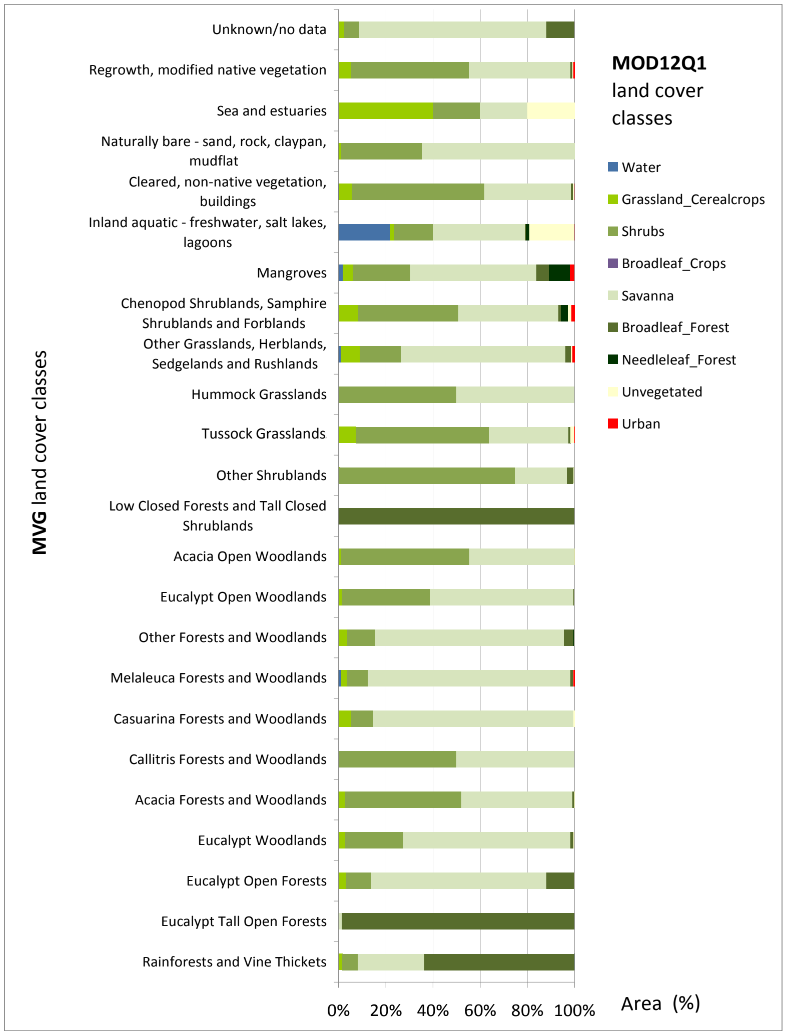

Fig. 4. Percentage area of NVIS MVG land cover classes within MOD12Q1 land cover classification for the BRC region.

Generally, the majority of the NVIS MVG woodland and grassland communities, ranging from “Eucalypt Open Forest” to “Acacia open Woodlands” and “Other Grasslands, Herblands, Sedgelands and Rushlands”, are represented as “Savanna” and/or “Shrubs” in the MOD12Q1 classification. The proportion of the MOD12Q1 class “Shrub” is higher in MVG NVIS classes of Woodlands and Shrublands dominated by Acacias, Callitris or in the classes “Hummock Grasslands”, “Tussock Grasslands”, and “Other Shrublands”. The NVIS MVG classes of Forest, such as “Low Closed Forests and Tall Closed Shrublands”, “Eucalypt Tall Open Forest”, and “Forests and Rainforests” were represented overwhelmingly by the MOD12Q1 class of “Broadleaf_Forest”. The NVIS MVG class “Sea and Estuaries” covers such a small proportion of the area of the BRC, that it is not listed in Table 3, where area percentages of classes have been rounded to two digits. That class is however to 40% classified as “Grassland_CerealCrops” by the MOD12Q1 (Fig. 4).

4.2 Comparison of the MODIS FPAR to the LANDSAT wFPC

A comparison of MODIS FPAR (1 km) 2004 dry seasonal statistics to a VSC classification (Table 2) of the 2004 Landsat wFPC image (25 m) is presented in Fig. 5 for the spatial extent of focal study site of the BBRs (about 9 500 km^2).

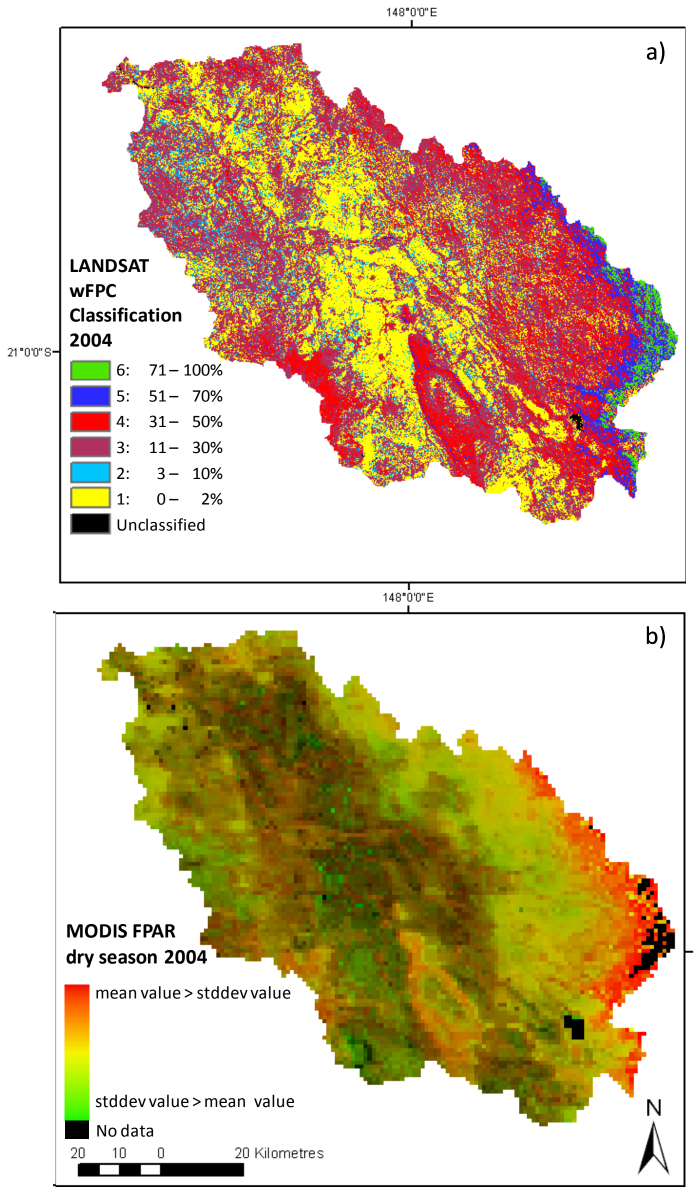

Fig. 5. a) top: VSC classes based on the Landsat wFPC image of the BBRs (25 m resolution) classified after Fensham et al. (2008) [65]; b) bottom: RGB composite of the 2004 dry season mean and standard deviation of MODIS FPAR for the BBRs (1 km resolution). (R: mean 2004 dry season MODIS FPAR; G: standard deviation 2004 dry season MODIS FPAR; B: empty).

Based on the concept of this additive color scheme the two MODIS FPAR dry seasonal statistics (Fig. 5b) reveal clear landscape patterns similar to the Landsat wFPC VSC classification (Fig. 5a). The higher the dry seasonal mean FPAR of a pixel, the brighter red it appears; the higher the dry seasonal FPAR standard deviation of a pixel, the greener it appears, whereas bright yellow shades refer to pixels with similar values for mean and standard deviation. River beds and densely or less densely vegetated areas, topographic features, for example, are easily distinguishable, despite the relatively coarse spatial resolution of the MODIS FPAR product. In Fig. 5b areas of high mean MODIS FPAR during this dry season correspond to areas of high wFPC in Fig. 5a (VSC classes 5 and 6, "Closed and Open Forests"). The densely forested eastern ranges of the BBRs are consistent with the relatively higher rainfall in that region. Areas with a higher standard deviation, i.e. temporal variability, than the mean MODIS FPAR over the 2004 dry season correspond to areas of lower wFPC; mainly VSC class 4, often mixed with classes 5, 2 and 1 (Table 2). Darker green shades in Fig. 5b correspond to the lowest wFPC values (VSC classes 1 and 2; Table 2). Less common in Fig. 5b are areas with yellow shades, which correspond to areas that over the dry season constantly absorb PAR. An example of this is VSC class 4 on eastern slopes, which consists of open woodlands with a distinct proportion of evergreen woody vegetation. These are savanna areas, which feature a highly seasonal grass understory. The pixels in the steepest eastern ranges in Fig. 5b (bottom) had no data values due to the strict quality control (see Fig. 2) and the presence of a dam in the southeast of the study site.

4.3 Relation of the MODIS FPAR to LANDSAT wFPC VSC classes

Descriptive statistics of the MODIS FPAR over the 2004 dry season were calculated for each VSC class (Fig. 6). The sensitivity of the global MODIS FPAR product to the VSC classes during one dry season was explored. The TVC is known to be less photosynthetically active and dominated by NPV or bare ground during this time. Figure 6 shows the values per VSC class in colors is equivalent to the class colors in Fig. 5a.

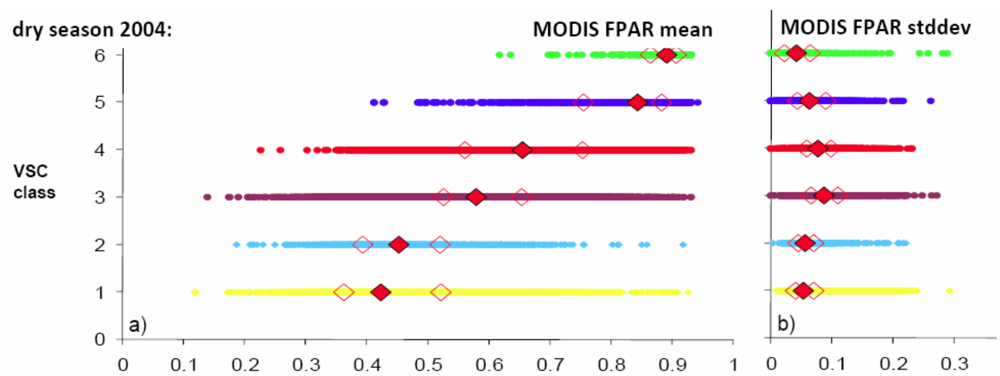

Fig. 6. MODIS FPAR 2004 dry seasonal mean (a), left) and standard deviation (b), right) ranges per VSC class (see Table 2 and Fig. 5) for the BBRs and its surrounding area (17179 km^2) (1 km pixel size). Red diamonds per class data range represent the median, orange hollow diamonds the upper and lower quartile respectively of the MODIS FPAR mean and standard deviation values in that class. Count of pixels per VSC class 1, 2, 3, 4, 5, and 6 in the MODIS FPAR image were n = 4869, 1236, 7666, 2262, 866, and 280 respectively.

Figure 6 shows a consistent pattern of increasingly higher median and reduced range for mean FPAR with increasingly denser and woodier VSC classes, i.e. the higher the wFPC (Fig. 6a). The differences amongst class means are statistically significant when analyzed in a one-sided ANOVA with $F(5, 16993) = 2326.26$ ($p < 0.001$) of the arcsine transformed mean values. The median values for the classes 1 to 6 dry seasonal MODIS FPAR mean increase from 0.42 to 0.89 respectively (Table 4).

Table 4. Summary of descriptive statistics of the MODIS FPAR mean for the dry season 2004 for the six VSC classes over the spatial extent of the BBRs and its surrounding area (17179 km^2) (1 km pixel size).

MEAN						
	cl1	***cl2***	***cl3***	***cl4***	***cl5***	***cl6***
Min	0.12	0.19	0.17	0.23	0.41	0.62
Max	0.93	0.92	0.9	0.93	0.94	0.93
Median	**0.42**	**0.45**	**0.58**	**0.66**	**0.84**	**0.89**
25th quartile	**0.36**	**0.39**	**0.52**	**0.56**	**0.75**	**0.86**
75th quartile	**0.52**	**0.52**	**0.65**	**0.75**	**0.88**	**0.91**
Stddev	0.13	0.1	0.1	0.13	0.1	0.05
Coefficient of variation	**0.28**	**0.21**	**0.17**	**0.20**	**0.13**	**0.06**

The MODIS FPAR standard deviation values per VSC class (Fig. 6b; right) reveal an additional pattern: the more structurally complex the classes are (i.e. classes 3 and 4), the higher their standard deviation in MODIS FPAR over that dry season. Class 3 "Woodland with shrubby understory, shrubland, Woodland" and class 4, "Open forest with shrubby understory" represent the structurally complex classes with increasing relevance of understory vegetation components. Median values for the standard deviation overall lie below 0.15 for all classes. The coefficient of variation (CV) represents a relative measure of variability per VSC class. VSC class 1 is clearly the most variable class (0.28), while VSC class 6 is the least variable (0.06). Despite high variability within and between each class, there is a general trend of decreasing CV with increasing VSC number (i.e. increasing wFPC; Table 2).

4.4 Comparison of the MODIS FPAR to the MODIS BGI

A comparison between the 20 coinciding MODIS FPAR observations for the 2001-2003 dry seasons and the MODIS BGI time-series is shown in Fig. 7. Measurements were averaged over selected homogenous regions (3-10 km^2) with less than 30% wFPC (see Fig. 5a).

A very good agreement between time trajectories of the global MODIS FPAR and the time trajectory of the regional MODIS BGI was found (Fig. 7). For 2001 to 2002, there is a general trend of increasing bare ground and decreasing FPAR. Figure 7 depicts the MODIS BGI scaled from 0 to 1, with 1 representing 100% bare ground. The global MODIS FPAR, scaled from 0 to 1, increases when MODIS BGI decreased and vice versa for homogenous regions within the VSC classes of wFPC of less than 30%. The wet season 2001/2002 is represented with small rise in MODIS FPAR value of about 0.1 as well as decrease in MODIS BGI value of about 0.05 most pronounced in the VSC class 3. All time trajectories reveal a response to the 2002/2003 wet seasonal rainfall (November to April the following year), with an increase of the MODIS FPAR for the VSC classes 1 and 2 of about 0.25, and for the VSC class 3 of 0.2. The MODIS BGI values decrease by about 0.2 for VSC classes 1 and 2, and decrease by less than 0.1 for VSC class 3. The year 2003 was a severely dry period on the 100 year record with less than average annual rainfall [51].

A linear regression between the times series of MODIS FPAR and BGI for the areas of wFPC under 30% is statistically significant ($\rho < 0.001$), with a correlation coefficient (R) of -0.428 for the classes 1 and 2, and of -0.685 for class 3 (Fig. 8).

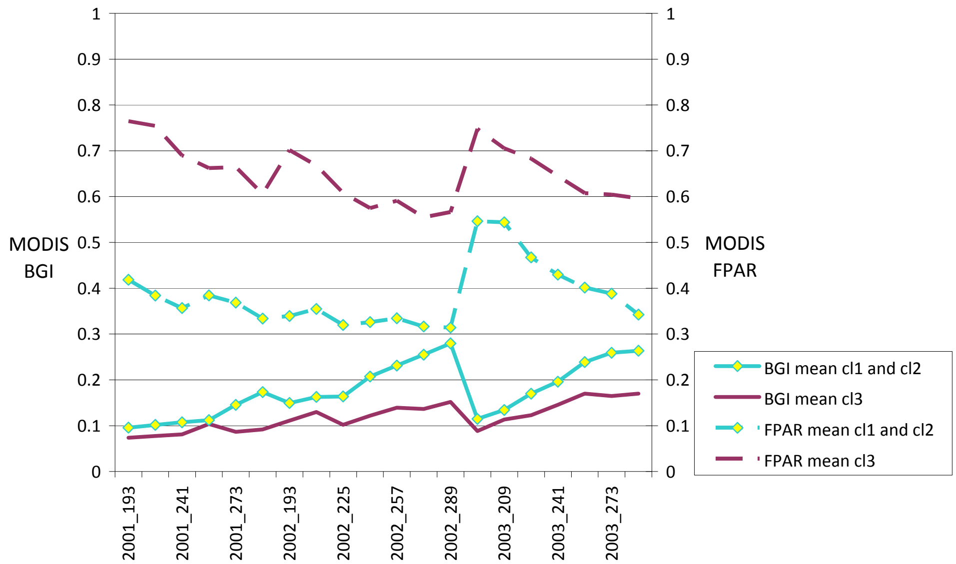

Fig. 7. Time series of MODIS FPAR mean (dashed lines) and MODIS BGI mean (solid lines) of the VSC classes 1 and 2 (cyan), and 3 (maroon) for coinciding dates of observations in the 2001 to 2003 dry seasons. The MODIS BGI is scaled from 0 to 1, with 1 representing 100% bare ground; the MODIS FPAR from 0 to 1, where 1 is maximum PAR absorption. The data was averaged over 20 selected homogenous regions within the VSC classes of wFPC below 30% (Table 2). The date of observation is given on the x-axis in 'year_day of year' (n = 20).

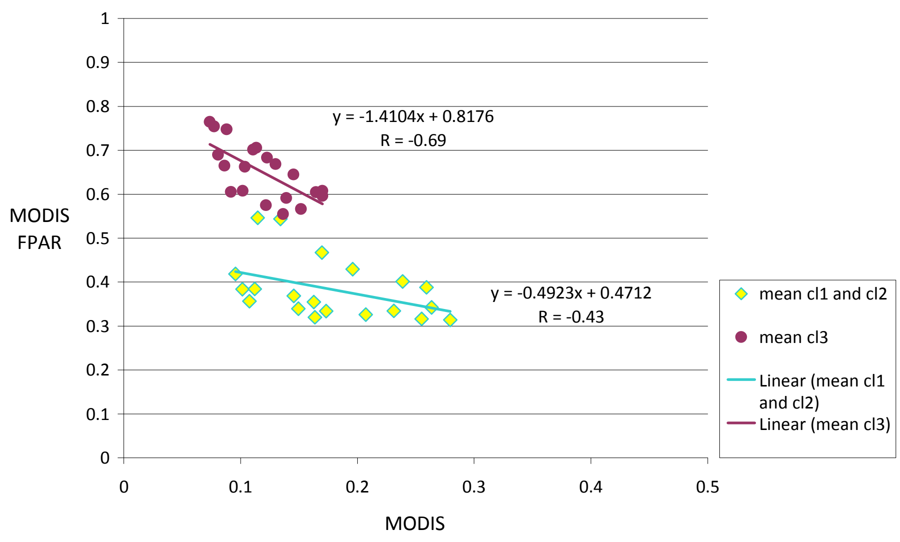

Fig. 8. Relation between the MODIS FPAR and BGI time-series values in the dry seasons of 2001 to 2003 for VSC classes 1 and 2 (cyan line) and 3 (maroon line). Values were averaged over the selected homogenous regions within the VSC classes where wFPC values are below 30% (Table 2); R represents the correlation coefficient (ρ< 0.001; n=20).

5 DISCUSSION

5.1 The MODIS FPAR

Amongst different biophysical variables of vegetation derived from remotely sensed imagery, fAPAR is of particular importance because it provides a direct connection between ecosystem structure and function [19]. The MODIS FPAR product is a high temporal resolution product that is free of charge; therefore it is a potentially valuable information source to complement remotely sensed information on TVC for our study site. Previous studies have shown that the absorption of PAR is sensitive to NPV components, structural vegetation groups [19], and that remotely sensed estimates of fAPAR are advantageous over classical vegetation indices particularly in heterogeneous landscapes [17, 41, 42]. Where open canopies feature a relevant understory component (PV or NPV) this can affect, and therefore co-determine, landscape and canopy fAPAR substantially [19, 43, 66].

The major limitations of the present study are linked to aspects of two MODIS FPAR inherent uncertainties. These are uncertainty in: (1) the input surface reflectances [60]; and (2) the algorithm underlying global land cover classification MOD12Q1 [24, 45], and (3) from the model used to build the look-up tables accompanying the algorithm [24, 60]. Our study addressed aspects of the MODIS FPAR limitation (1) and (2). To investigate the validity of the model used to build the look-up tables accompanying the MODIS FPAR algorithm (3) was beyond the scope of this study.

(1) Average uncertainties for reflectances of highest quality in the red and near-infrared bands of MODIS surface reflectances lie between 10-15% [42, 67], the only two bands to date being used in the MODIS FPAR C4 algorithm [42]. In dry savanna ecosystem the MODIS FPAR C4 retrievals have been shown to overestimate field based measurements of PAR by 8-20% [42], whereas techniques to measure PAR in the field might have accounted for some of the bias [41, 45]. Hence it is suggested, that the user community worldwide would benefit from the development of a common field protocols. The quality of FPAR retrievals was maximized through a strict quality control of the MODIS FPAR time series, rejecting FPAR retrievals by the back-up algorithm. This reduces the introduction of error resulting from the dependence of the NDVI to fAPAR relationship on canopy structure (leaf angle distribution, vegetation clumping, leaf and branch optical properties) and land cover [17, 19, 43]. Resulting gaps in MODIS FPAR time series occurred mostly in the eastern ranges and highly forested areas in the BBRs which encounter frequent cloud cover even over the dry season (Fig. 2). It is further a known deficiency of the MODIS reflectance values that they can saturate in areas of broadleaf forests, like these eastern ranges in the BBRs (see Fig. 3) [24, 45]. Filling the quality controlled time series was beyond the scope of this study; however the recently released MODIS FPAR C5 product may reduce the need for this [68].

(2) A comparison of a smaller number of biomes from the MOD12Q1 to structurally and floristically determined land cover classes from the NVIS MVG does not surprisingly result in several discrepancies. Differences in the underlying MOD12Q1 biome classification to a more detailed regional land cover classification could potentially introduce a large error in retrieved FPAR at the native resolution of the MODIS FPAR product. Distinctly different canopy structures will affect the three-dimensional radiation field [44]. It is clear that the MOD12Q1 has not been designed to capture the spatial variation in structure present in floristically unique Australian forests. However, at the regional scale of the study site, our comparison showed a reasonable correspondence for the dominant classes, in terms of area. Both classifications largely categorized the BRC as dominated by vertically complex and heterogeneous canopies (Table 3). Therefore a complex three dimensional RTM for the FPAR retrievals is invoked [46]. To investigate this was the main reason for the way the comparison was conducted here. Discrepancies

in the global MOD12Q1 biome classification were detected, but in many cases the replacement classes in the MOD12Q1 are likely be spectrally and structurally similar to the NVIS MVG classes (see Fig. 4).

Investigating limitations in the MODIS FPAR product has maximized the overall utility of the MODIS FPAR values for the study site. The insight gained into uncertainties in the underlying biome classification will benefit subsequent analysis of MODIS FPAR for regional application.

In the process of this study a limitation to the MODIS FPAR C4 product algorithm was identified as a deviating from the original algorithm (pers. comm. Yuri Knyazikhin, 18.11.2008): MODIS FPAR C4 provides FPAR retrievals under diffuse illumination conditions [61]. Diffuse illumination conditions enhance PAR absorption at the leaf and canopy level more than under angular illumination conditions in areas where plants with erectophile leaves dominate (such as grasses, eucalypts or acacias) and with lower plant area index [10, 35]. These environmental conditions (erectophile leaves and low PAI) occur in more than 70% of our study area. Therefore, we expected the MODIS FPAR C4 product to have retrieved higher estimates of FPAR than the C5 product under direct illumination conditions. This was confirmed in a comparison of C4 and C5 MODIS FPAR for the study area (results not shown here). Our study only used the MODIS FPAR C4 to conduct empirical comparisons with other TVC and VSCs. There was no comparison of FPAR quantities and the differences between the estimates are minor, therefore we concluded this would have a negligible impact on our results (pers. comm. Yuri Knyazikhin, 18.11.2008). We also recognize known limitations to the MODIS temporal resolution, which render it incapable to account for diurnal variations of fAPAR due to changes in solar zenith angle. These changes have been shown to peak around midday, and exhibit diurnal amplitudes that exceed 0.1 to 0.15 [35]. The value of this amplitude is equal to the margin of uncertainty of FPAR retrievals [41] and due to the morning overpass of the TERRA delivering the MODIS FPAR C4 daily maximum absorbed PAR of the canopy might be underestimated. To counterbalance potential MODIS FPAR spatial inaccuracies, our study uses test areas of more than three up to five pixels in size.

5.2 Relation of the MODIS FPAR to the regionally developed total vegetation and land cover products

We decided to explore the relation of the global MODIS FPAR to regionally developed TVC products Landsat wFPC and MODIS BGI, because they have been developed and tested for their performance specifically for the Australian climatic, floristic and structural conditions. To show how the global, quality controlled MODIS FPAR relates to these regional products in respect of vegetation structure and the biophysical property of PAR absorption the focus of this study was put on dry seasons in the dry-tropical research area. The rationale for this approach was that during this point of the hydrological year the TVC is typically abundant with NPV (e.g., dry grass, leaf litter, and woody material) or bare ground components. NPV as well as PV TVC components have been demonstrated to absorb PAR elsewhere in similar ecosystems at landscape and canopy level [e.g. 19]. Thus, if MODIS FPAR would prove to be sensitive to TVC structure and components of varying wFPC levels, it could assist in determining factors relevant for erosion modelling of the following wet seasonal rainfall events.

Known sources of uncertainties in the presented results inherent to the MODIS FPAR product have been discussed above (5.1). Potential sources of uncertainties inherent to the methodology of the comparison in this study are restricted to the assumption that: (i) the VSC classification is representative of the areas major structural and floristic characteristics (Table 2, Fig. 5), and (ii) observed variability and dispersion of the global MODIS FPAR statistics (Fig. 5 - 8) result from a combination of spatio- and temporally variable factors: the natural complexity of vertically and horizontally heterogeneous VSC, and/or the composition of PV and NPV TVC components, climate, soil condition, land management practices, and potential disturbances (fire or clearing).

From our point of view, the (i) representativeness and structural homogeneity of the VSC classes is reflected by the overall low values of standard deviation of all VSC classes, which lie below 0.1 (Fig. 6), approaching the MODIS FPAR products accuracy range. This is not surprising, as the classification into VSC was based on information tailored to the structural and floristic conditions in the study area [26, 65]. Observed patterns in variability and dispersion of MODIS FPAR statistics (ii) over dry seasons for all VSC classes are in accordance with known structural characteristics and biophysically driven behaviour for this type of VSC [35, 41]. The natural complexity of the VSC over the dry season seemed, in agreement to reported PAR absorption in heterogeneous, dry landscapes or by different tree species, and agree with studies on the global MODIS FPAR product [19, 69, 70] and with field and model experiments shown elsewhere [19, 43, 71]. Generally, the lower the wFPC cover, the lower are the mean and larger the CV of the MODIS FPAR observations over the selected dry season (Fig. 6 and Table 4). Only VSC class 4, "Open forest with shrubby understory" had a higher variability (CV of 0.20) than class 3 of Woodlands. This could be attested to the fact that the understory in the common Eucalypt Woodlands (such as class 3) varies from grasses to shrubs, but have in some cases attained a parkland appearance due to frequent fire and grazing [64]. This parkland, and hence more homogenous, appearance has been described to typify Woodlands in the eastern parts of Australia [64]. The VSC class 1 was clearly the most variable class (CV of 0.28), which might manifest spatially (i.e. discontinuities in bare ground) and temporally (rapid responses to any rainfall). Despite this convincing contextual explanation, the results showing the dispersion of MODIS FPAR means and standard deviation of the VSC classes, however, have to be interpreted carefully. The results could simply confirm what was to be expected when analysing proportional data such as the MODIS FPAR: classes in the mid ranges (class 4 and 3) could demonstrate a higher standard deviation as a feature of the type of data, rather than the underlying biophysical processes and TVC components. An upcoming study will hence investigate the impact of measured PV and NPV components on the dispersion of MODIS FPAR means and standard deviations of the VSC classes.

The analysis of the MODIS FPAR and MODIS BGI comparison for selected homogenous areas of low wFPC provided results, however, clearly suggest that the composition of the TVC components, PV and NPV, has had an impact on the MODIS FPAR signal in our study (Fig. 7). Vegetation in areas of lower wFPC during the dry seasons is mostly comprised of herbaceous vegetation, grasslands, potentially high bare ground components, some features of open woodland and shrublands. The impact of NPV components on the MODIS FPAR signal is reflected in the statistically significant correlation between the MODIS FPAR and MODIS BGI coinciding observations from 2001-2003 for homogenous areas of wFPC below 30% (Fig. 8). The weaker correlation coefficient of -0.428 between both products for the classes 1 and 2 could be indicative of classes 1 and 2 being more structurally different and possibly separable through the MODIS FAPR (Fig. 8). The dry seasonal time trajectories MODIS FPAR and the MODIS BGI for the selected homogenous areas (Fig. 7 and 8), can be interpreted to mirror the effect of spatio-temporal rainfall patterns on the observed PAR absorption and resulting MODIS FPAR signal. During the period of comparison from 2001 to 2003 both of the two wet seasons, 2001/2002 and 2002/2003, featured the similar amount of below average rainfall in the subcatchment: the trajectories of both products show differently strong amplitude for the following dry seasons. In absence of known other factors affecting the observed PAR absorption/FPAR signal and BGI values, this difference is likely to be the result of local variations in rainfall patterns [47]. We here acknowledge potential effects of the soil condition on the variability of the MODIS FPAR signal which provide a wide field for further investigations [10]. Little detailed soil information for the study area to date and the defined scope of the study prohibited us to address this issue here.

5.3 Remotely sensed biophysical properties in heterogeneous landscapes – general remarks

Modelling of the radiation regime of a mixture of vegetation species is still acknowledged to be a major challenge, if not a fundamental problem, of the Earth's land remote sensing and climate applications [49, 72]. There are still substantial deficiencies in existing mixture RTM. For once, species and species dependent structural, optical, and biophysical properties are often ignored in general. Secondly, the fact that species radiation could be a function of coupled radiation when multiple scattering of photons occurs [72] has to be acknowledged. And, if spatial clumping of species is in turn completely neglected the coupling can also be overestimated, causing deficiencies of the mixture RTM [72]. Shabanov et al. (2007) [72] offer a first theoretical basis for future mixture model applications accounting for the above mentioned deficiencies.

In practice, higher quality land cover classifications accounting for species or at least vegetation category dependent structural, optical and biophysical characteristics are vital for improving existing mixture RTM for the derivation of biophysical variables. To estimate the canopy radiation regime, three main important features have long been known [44]: (1) the architecture of individual plants or trees and the entire canopy; (2) optical properties of vegetation elements (leaves, stems) and ground; the former depends on physiological conditions (water status, pigment concentration); and (3) atmospheric conditions which determine the incident radiation field. In relation to (1) it is well known that the heterogeneity of the plant canopy can be described by three-dimensional leaf area distribution functions, which values vary spatially and depend on factors, such as trunk distribution, topography, stem-trunk-branch area fraction, foliage dispersion, leaf and crown size, and leaf clumping [44]. Huemmrich et al (2005) [41] emphasize the relevance of factors describing heterogeneous plant canopies for African Kalahari Woodlands, a similar ecosystem like this study area. In this light, we suggest that an improved adaptation of an underlying biome classification and specific consideration in the RTMs for MODIS and general FPAR retrievals to the unique floristic characteristics in the Australian environment is desirable. In relation to the second main feature mentioned above to estimate canopy radiation regimes, (2) optical properties of vegetation elements and ground, we consider the temporal variability of the species-light interaction and ecosystem dependent characteristics a major challenge for remote sensing applications. This temporal variability is dependent on physiological conditions and partly on light illumination conditions, and thus capable to vary at diurnal scale [34], a temporal resolution not yet reached by today's remotely sensed products.

In summary, the need for increased and operational spectral, temporal, and spatial resolution of operational remotely sensed data and more continuous, complex, though affordable field validation is justifiably still regarded as the foremost challenge for the retrieval of remotely sensed, biophysical vegetation properties. While we acknowledge these challenges, we saw the exploration of an existent operational, global product in a regional application as one small step towards these directions. Further improvements in technological and theoretical developments will continue to benefit the modelling of canopy radiation regimes and hence practical applications of remotely sensed TVC mapping and monitoring, particularly in heterogeneous landscapes and remote areas (such as HySPIRI, MISR [17-19], or radar applications).

6 CONCLUSIONS AND FUTURE WORK

This study compared the global MODIS FPAR product (C 4) and its underlying global MOD12Q1 biome classification related to (i) national/regional classification of major vegetation groups (NVIS MVG), and (ii) to regionally developed Landsat and MODIS products of woody foliage projective and bare ground cover in a subtropical river catchment in Queensland, Australia. A thorough processing with a strict quality control of the MODIS FPAR data and examination of the algorithm underlying global MOD12Q1 biome classification were conducted prior to the comparison to regionally developed remotely sensed Landsat and MODIS products. The MOD12Q1 was found to be in certain agreement in the association of structurally similar MOD12Q1 biomes to the NVIS MVG classes for about 94% of the 140 000 km^2 of the study area. Despite discrepancies in number of classes, and lack of incorporation of the regional faunal attributes, the global MOD12Q1 biome classification was considered an acceptable representation of the study area's major vegetation groups. The NVIS MVG classes of forests and woodlands are classified as structurally similar biomes in the MOD12Q1, which were "Savanna" and "Shrubs". Due to the MOD12Q1 representing biomes rather than structural and floristic vegetation communities and the fact that the BRC study area is dominated by savannas [73], this can is however considered a reasonable match. For the dominant biomes the MOD12Q1 delivers complex structural and angular characteristics for the use in the RTM embedded in the MODIS FPAR retrieval algorithm in the study area.

Major findings of the consecutive comparison of the MODIS FPAR to the Landsat and MODIS TVC products included, that the quality controlled time series of 1 km, 8-day composites of the global MODIS FPAR:

- provided time trajectories of assumed PAR absorption in homogenous and representative areas of low wFPC (less than 30%) during dry seasons, which were strongly, inversely related to the regionally developed MODIS BGI (500 m resolution) product (20 coinciding observations from 2001 to 2003) ($\rho < 0.001$) with R-values of -0.69 and -0.43 (Fig. 7 and 8).
- revealed statistically significant differences in means of VSC classes from a 2004 Landsat wFPC image (resampled from 25m to 1km resolution) over one dry season (2004) in the subcatchment area (17179 km^2) (Fig. 6) with $F(5, 16718) = 2429.47$, $p < 0.001$. Expected, VSC-class specific variability and dispersion in PAR absorption was well expressed through descriptive statistics of the MODIS FPAR (Table 4), with CV increasing with decreasing wFPC proportions.
- represented characteristic landform and vegetation patterns at subcatchment scale (9500 km^2), very similar to the ones depicted by a classification of the regional, annual LANDSAT wFPC (2004, 25 m resolution) product into VSC (Fig. 5). Visual interpretation based on an additive color scheme using a false color composite of 2004 dry season MODIS FPAR mean and standard deviation suggested that topographic and climatic patterns of the subcatchment were mirrored clearly, and more detailed than in the MODIS FPAR underlying MOD12Q1 classification (Fig. 3).

The results presented here for all VSC classes of varying levels of wFPC in dry seasons suggest that different vegetation layers in vertically and horizontally heterogeneous landscapes contribute to the PAR absorption measured by the MODIS FPAR product. Asner (2000) and Olofsson et al. (2007) have earlier pointed to the relevance of understory components in canopy PAR absorption [40, 43]. As areas of less than 30% wFPC in a dry season of the study area have an abundance of NPV components in their TVC, the MODIS FPAR also seemed to be sensitive to NPV components. The results are in agreement with findings that the contribution of NPV components to canopy and landscape PAR absorption can be substantial at varying spatial levels (from canopy to landscape), as demonstrated in savannas [44] or shortgrass ecosystems [19]. This variability and change expressed through MODIS FPAR values/PAR absorption can be understood to be driven by differences in the biophysical behavior of the local TVC components (including PV, bar ground and NPV) responding to climate or land management factors [35, 41]. To identify driving factors of the MODIS FPAR signal an upcoming paper will decompose the PV, NPV, and bare soil components based on field data, fractional Landsat data from spectral mixture analysis, both from the QDERM.

Based on the presented results, known limitations and advantages of the MODIS FPAR and known results from other fAPAR studies, our study suggest that future development and improvement of remotely sensed fAPAR products would benefit from: (i) long term field observations of leaf level-variables complementing canopy-level variables above and below the canopy, and (ii) improved field protocols for measuring PAR absorption worldwide, as e.g. Zhang et al. (2005) similarly suggest [74]. Despite promising results from this study, we further advocate the adaptation of algorithms to derive biophysical parameters, such as fAPAR, to the unique Australian, or a least to southern hemispheric floristic and structural conditions. That is particularly relevant for areas classified by the MOD12Q1 as deciduous broadleaf forests, where the MOD15A2 algorithm assumes constant standard leaf optical properties throughout the entire plant growing season. The adaptation of underlying biome classifications to regionally relevant VSC classes is also relevant for any further quantitative studies on PAR absorption and photosynthetic activity or light use efficiency at canopy and landscape scale, as they are affected by canopy structure (such as clumping and leaf inclination) and by different vertical layers [32, 75].

However, there is strong evidence for the value of the high temporal resolution MODIS FPAR for further exploration and validation to derive TVC estimates in our study area for ecophysiological models and e.g. erosion models. The MODIS FPAR C 5 product has been recently released and will address several limitations of the C 4, while further developments could lead to the inclusion of an increased number of MODIS reflectance bands used in the FPAR algorithm. In combination with field observations, which require the understanding and measuring of not only biophysical, but structural properties of TVC, high quality, repeatable, synoptic-scale remote sensing estimates of fAPAR will play an increasingly essential role: a) as means for extrapolating ecophysiological measurements, and b) in linking fAPAR estimates successfully to other functional attributes of ecosystems, such as CO2 assimilation, net primary production, and water loss [19, 76].

Acknowledgments

This study is funded through a University of Queensland Research Scholarship and additionally supported by CSIRO Land and Water, Canberra, in particular Dr Arnold Dekker. The authors would like to thank Dr Edward King and Matthew Paget, CSIRO, for the provision and the support with the MODIS FPAR product, Dr Peter Scarth from the Remote Sensing Group of the QDERM for their data supply and advice. We would like to acknowledge the helpful personal communication with Dr Yuri Knyazikhin, Dr Mark Friedl of the MODIS land product team, and Dr Gabriela Schaepman-Strub. We appreciate that recent documentation of activities related to the new MODIS FPAR collection 5 and its new underlying biome classification have become more transparent than in the beginning of this study. We would like to thank John Armston for his relevant input to improve this document and the anonymous reviewers for their constructive comments.

References

[1] K. A. Galvin, R. S. Reid, J. Behnke, R.H., and N. T. E. Hobbs, *Fragmentation in Semi-Arid and Arid Landscapes: Consequences for Human and Natural Systems*, Springer, Dordrecht, The Netherlands (2008).

[2] M. M. Cole, *The Savannas: biogeography and geography*, United States ed., Academic Press Inc., Orlando, FL (1986).

[3] G. P. Asner, A. J. Elmore, L. P. Olander, R. E. Martin, and A. T. Harris, "Grazing Sytstems, Ecosystem Responses, and Global Change," *Annu. Rev. Environ. Res.* **29(**1), 261-299 (2004) [doi: 10.1146/annurev.energy.29.062403.102142].

[4] C. Folke, S. Carpenter, B. Walker, M. Scheffer, T. Elmqvist, L. Gunderson, and C. S. Holling, "Regime shifts, resilience, and biodiversity in ecosystem management," *Annu. Rev. Ecol. Evol. Systematics* **35(**1), 557-581 (2004) [doi: 10.1146/annurev.ecolsys.35.021103.105711].

[5] J. Grace, J. San José, P. Meir, H. S. Miranda, and R. A. Montes, "Productivity and carbon fluxes of tropical savannas," *J. Biogeogr.* **33(**3), 387-400 (2006) [doi:10.1111/j.1365-2699.2005.01448.x].

[6] P. Scarth, M. Byrne, T. Danaher, B. Henry, R. Hasset, J. O. Carter, and P. Timmers, "State of the paddock: monitoring condition and trend in groundcover across Queensland," presented at *13th Australasian Remote Sensing & Photogrammetry Conference (ARSPC),* 20 – 24 November, Canberra, ACT, Australia, 2006.

[7] Queensland Dept. of Natural Resources and Water, "Delbessie Agreement: state rural leasehold land strategy," Dept. of Natural Resources and Water, Brisbane, Queensland, Australia, (2007).

[8] Queensland Department of Premier and Cabinet, "The Reef Water Quality Protection Plan (RWQPP)," Department of Premier and Cabinet,Queensland, Brisbane, Queensland, Australia, (2003).

[9] G. S. Okin, "Relative spectral mixture analysis - A multitemporal index of total vegetation cover," *Remote Sens. Environ.* **106(**4), 467-479 (2007) [doi: 10.1016/j.rse.2006.09.018].

[10] Y. Tian, R. E. Dickinson, L. Zhou, X. Zeng, Y. Dai, R. B. Myneni, Y. Knyazikhin, X. Zhang, M. Friedl, H. Yu, W. Wu, and M. Shaikh, "Comparison of seasonal and spatial variations of leaf area index and fraction of absorbed photosynthetically active radiation from Moderate Resolution Imaging Spectroradiometer (MODIS) and Common Land Model," *J. Geoph. Res. D: Atmospheres* **109**, 15 (2004) [doi: 10.1029/2003JD003777].

[11] R. Houborg, H. Soegaard, and E. Boegh, "Combining vegetation index and model inversion methods for the extraction of key vegetation biophysical parameters using Terra and Aqua MODIS reflectance data," *Remote Sens. Environ.,* **106(**1), 39-58 (2007) [doi: 10.1016/j.rse.2006.07.016].

[12] C. B. Field, J. T. Randerson, and C. M. Malmström, "Global net primary production: Combining ecology and remote sensing," *Remote Sens. Environ.* **51(**1), 74-88 (1995) [doi: 10.1016/0034-4257(94)00066-V].

[13] S. Ustin, L., *Manual Of Remote Sensing / Remote Sensing For Natural Resource Management And Environmental Monitoring*, 3rd ed. vol. 4, Wiley, Hoboken, NJ (2004).

[14] P. J. Sellers, B. W. Meeson, F. G. Hall, G. Asrar, R. E. Murphy, R. A. Schiffer, F. P. Bretherton, R. E. Dickinson, R. G. Ellingson, C. B. Field, K. F. Huemmrich, C. O. Justice, J. M. Melack, D. S. Schimel, P. D. Try, and N. T. Roulet, "Remote Sensing

of the Land Surface for Studies of Global Change: Models - Algorithms - Experiments," *Remote Sens. Environ.* **51(**1), 3-26 (1995) [doi: 10.1016/0034-4257(94)00061-Q].

[15] C. J. Tucker, C. L. Vanpraet, M. J. Sharman, and G. Van Ittersum, "Satellite remote sensing of total herbaceous biomass production in the senegalese sahel: 1980-1984," *Remote Sens. Environ.* **17(**3), 233-249 (1985) [doi: 10.1016/0034-4257(85)90097-5].

[16] G. M. Lodge and S. R. Murphy, "Ground cover in temperate native perennial grass pastures. II. Relationship with herbage and litter mass," *Rangeland J.* **24(**2), 301-312 (2002) [doi: 10.1071/RJ02017].

[17] W. J. D. van Leeuwen and A. R. Huete, "Effects of standing litter on the biophysical interpretation of plant canopies with spectral indices," *Remote Sens. Environ.* **55(**2), 123-138 (1996) [doi: 10.1016/0034-4257(95)00198-0].

[18] A. R. Huete and R. D. Jackson, "Suitability of spectral indices for evaluating vegetation characteristics on arid rangelands," *Remote Sens. Environ.* **23(**2), 213-232, IN1-IN8 (1987) [doi: 10.1016/0034-4257(87)90038-1].

[19] G. P. Asner, C. A. Wessman, and S. Archer, "Scale dependency of Absorption of Photosynthetically Active Radiation in terrestrial ecosystems," *Ecol. Appl.* **8(**4), 1003-1021 (1998) [doi: 10.1890/1051-0761(1998)008[1003:SDOAOP]2.0.CO;2].

[20] G. P. Asner and C. A. Wessman, "Scaling PAR absorption from the leaf to landscape level in spatially heterogeneous ecosystems," *Ecol. Model.* **103(**1), 81-97 (1997) [doi: 10.1016/S0304-3800(97)00080-X].

[21] J. D. Armston, R. J. Denham, T. J. Danaher, P. F. Scarth, and T. N. Moffiet, "Prediction and validation of foliage projective cover from Landsat-5 TM and Landsat-7 ETM+ imagery," *J. Appl. Remote Sens.* **3(**1), 033540-28 (2009) [doi: 10.1117/1.3216031].

[22] T. Gill and S. Phinn, "Estimates of bare ground and vegetation cover from Advanced Spaceborne Thermal Emission and Reflection Radiometer (ASTER) short-wave-infrared reflectance imagery," *J. Appl. Remote Sens.* **2**, 023511 (2008) [doi: 10.1117/1.2907748].

[23] R. D. Graetz, R. P. Pech, and A. W. Davis, "The Assessment and Monitoring of Sparsely Vegetated Rangelands Using Calibrated Landsat Data," *Int. J. Remote Sens.* **9(**7), 1201-1222 (1988) [doi: 10.1080/01431168808954929].

[24] M. J. Hill, U. Senarath, A. Lee, M. Zeppel, J. M. Nightingale, R. J. Williams, and T. R. McVicar, "Assessment of the MODIS LAI product for Australian ecosystems," *Remote Sens. Environ.* **101(**4), 495-518 (2006) [doi: 10.1016/j.rse.2006.01.010].

[25] Department of Natural Resources and Water, "Land cover change in Queensland 2004–2005: a Statewide Landcover and Trees Study (SLATS) Report," Department of Environment and Resource Management, Brisbane, 1-88 (2007).

[26] R. L. Specht and A. Specht, *Australian Plant Communities: Dynamics of Structure, Growth and Biodiversity*, Oxford University Press, Oxford (1999).

[27] T. K. Gill, S. R. Phinn, J. D. Armston, and B. A. Pailthorpe, "Estimating tree-cover change in Australia: challenges of using the MODIS vegetation index product," *Int. J. Remote Sens.* **30(**6), 1547 - 1565 (2009) [doi: 10.1080/01431160802509066].

[28] H. Lu, M. R. Raupach, T. R. McVicar, and D. J. Barrett, "Decomposition of vegetation cover into woody and herbaceous components using AVHRR NDVI time series," *Remote Sens. Environ.* **86(**1), 1-18 (2003) [doi: 10.1016/S0034-4257(03)00054-3].

[29] J. Milne, P. Scarth, and J. Armston, "Predictions of total standing dry matter in tropical savannah grasslands using MODIS satellite imagery," presented at *Australasian Remote Sensing and Photogrammetry Conference (ARSPC)*, 29th of September - 3rd of October, Darwin, NT, 2008.

[30] J.-P. Guerschman, M. J. Hill, L. J. Renzullo, D. J. Barrett, A. S. Marks, and E. Botha, "Estimating fractional cover of photosynthetic vegetation, non-photosynthetic vegetation and bare soil in the Australian tropical savanna region upscaling the EO-1 Hyperion and MODIS sensors," *Remote Sens. Environ.* **113(**5), 928-945 (2009) [doi: 10.1016/j.rse.2009.01.006].

[31] C. S. T. Daughtry, E. R. Hunt, and J. E. McMurtrey III, "Assessing crop residue cover using shortwave infrared reflectance," *Remote Sens. Environ.* **90**, 126-134 (2004) [doi: 10.1016/j.rse.2003.10.023].

[32] Q. Zhang, X. Xiao, B. Braswell, E. Linder, S. Ollinger, M. L. Smith, J. P. Jenkins, F. Baret, A. D. Richardson, B. Moore, and R. Minocha, "Characterization of seasonal variation of forest canopy in a temperate deciduous broadleaf forest, using daily MODIS data," *Remote Sens. Environ.* **105(**3), 189-203 (2006) [doi: 10.1016/j.rse.2006.06.013].

[33] X. Le Roux, H. Gauthier, A. Begue, and H. Sinoquet, "Radiation absorption and use by humid savanna grassland: assessment using remote sensing and modelling," *Agric. For. Meteorol.* **85(**1), 117-132 (1997) [doi: 10.1016/S0168-1923(97)00002-6].

[34] V. Thomas, D. A. Finch, J. H. McCaughey, T. Noland, L. Rich, and P. Treitz, "Spatial modelling of the fraction of photosynthetically active radiation absorbed by a boreal mixedwood forest using a lidar-hyperspectral approach," *Agric. For. Meteorol.* **140(**1-4), 287-307 (2006) [doi: 10.1016/j.agrformet.2006.04.008].

[35] Y. Nouvellon, A. Bégué, M. Susan Moran, D. L. Seen, S. Rambal, D. Luquet, G. Chehbouni, and Y. Inoue, "PAR extinction in shortgrass ecosystems: effects of clumping, sky conditions and soil albedo," *Agric. For. Meteorol.* **105(**1-3), 21-41 (2000) [doi: 10.1016/S0168-1923(00)00194-5].

[36] N. Gobron, B. Pinty, M. Taberner, F. Mélin, M. M. Verstraete, and J. L. Widlowski, "Monitoring the photosynthetic activity of vegetation from remote sensing data," *Adv. Space Res.* **38(**10), 2196-2202 (2006) [doi: 10.1016/j.asr.2003.07.079].

[37] Y. Knyazikhin, J. Martonchik, D. Diner, R. B. Myneni, M. Verstraete, B. Pinty, and N. Gobron, "Estimation of vegetation canopy leaf area index and fraction of absorbed photosynthetically active radiation from atmosphere-corrected MISR data," *J. Geoph. Res. D: Atmospheres* **103 (**24), 32239-32256 (1998) [doi: 10.1029/98JD02461].

[38] G. Asrar, R. B. Myneni, and B. J. Choudhury, "Spatial heterogeneity in vegetation canopies and remote sensing of absorbed photosynthetically active radiation: A modeling study," *Remote Sens. Environ.* **41(**2-3), 85-103 (1992) [doi: 10.1016/0034-4257(92)90070-Z].

[39] D. P. Turner, W. D. Ritts, W. B. Cohen, S. T. Gower, S. W. Running, M. Zhao, M. H. Costa, A. A. Kirschbaum, J. M. Ham, S. R. Saleska, and D. E. Ahl, "Evaluation of MODIS NPP and GPP products across multiple biomes," *Remote Sens. Environ.* **102(**3-4), 282-292 (2006) [doi: 10.1016/j.rse.2006.02.017].

[40] G. P. Asner, C. A. Wessman, C. A. Bateson, and J. L. Privette, "Impact of tissue, canopy, and landscape factors on the hyperspectral reflectance variability of arid ecosystems," *Remote Sens. Environ.* **74(**1), 69-84 (2000) [doi: 10.1016/S0034-4257(00)00124-3].

[41] K. F. Huemmrich, J. L. Privette, M. Mukelabai, R. B. Myneni, and Y. Knyazikhin, "Time-series validation of MODIS land biophysical products in a Kalahari woodland, Africa," *Int. J. Remote Sens.* **26(**19), 4381-4398 (2005) [doi: 10.1080/01431160500113393].

[42] R. Fensholt, I. Sandholt, and M. S. Rasmussen, "Evaluation of MODIS LAI, fAPAR and the relation between fAPAR and NDVI in a semi-arid environment using in situ measurements," *Remote Sens. Environ.* **91(**3-4), 490-507 (2004) [doi: 10.1016/j.rse.2004.04.009].

[43] P. Olofsson and L. Eklundh, "Estimation of absorbed PAR across Scandinavia from satellite measurements. Part II: Modeling and evaluating the fractional absorption," *Remote Sens. Environ.* **110(**2), 240-251 (2007) [doi: 10.1016/j.rse.2007.02.020].

[44] Y. Knyazikhin, J. Glassy, J. L. Privette, Y. Tian, A. Lotsch, Y. Zhang, Y. Wang, J. T. Morisette, P. Votava, R. B. Myneni, R. R. Nemani, and S. W. Running, "MODIS Leaf Area Index (LAI) and Fraction of Photosynthetically Active Radiation Absorbed by Vegetation (FPAR) Product (MOD15) Algorithm Theoretical Basis Document," NASA Goddard Space Flight Center, Greenbelt, MD (1999).

[45] D. C. Steinberg, S. J. Goetz, and E. J. Hyer, "Validation of MODIS FPAR products in boreal forests of Alaska," *IEEE Trans. Geosci. Remote Sens.* **44(**7), 1818-1828 (2006) [doi: 10.1109/TGRS.2005.862266].

[46] W. Yang, B. Tan, D. Huang, M. Rautiainen, N. V. Shabanov, Y. Wang, J. L. Privette, K. F. Huemmrich, R. Fensholt, I. Sandholt, M. Weiss, D. E. Ahl, S. T. Gower, R. R. Nemani, Y. Knyazikhin, and R. B. Myneni, "MODIS Leaf Area Index Products: From Validation to Algorithm Improvement," *IEEE Trans. Geosci. Remote Sens.* **44(**7), 1885-1898 (2006) [doi: 10.1109/TGRS.2006.871215].

[47] D. E. Ahl, S. T. Gower, S. N. Burrows, N. V. Shabanov, R. B. Myneni, and Y. Knyazikhin, "Monitoring spring canopy phenology of a deciduous broadleaf forest using MODIS," *Remote Sens. Environ.* **104(**1), 88-95 (2006) [doi: 10.1016/j.rse.2006.05.003].

[48] W. Yang, D. Huang, B. Tan, J. C. Stroeve, N. V. Shabanov, Y. Knyazikhin, R. N. Ramakrishna, and R. B. Myneni, "Analysis of Leaf Area Index and Fraction of PAR Absorbed by Vegetation Products From the Terra MODIS Sensor: 2000–2005," *IEEE Trans. Geosci. Remote Sens.* **44(**7), 1829-1842 (2006) [doi: 10.1109/TGRS.2006.871214].

[49] N. V. Shabanov, Y. Wang, W. Buermann, J. Dong, S. Hoffman, G. R. Smith, Y. Tian, Y. Knyazikhin, and R. B. Myneni, "Effect of foliage spatial heterogeneity in the MODIS LAI and FPAR algorithm over broadleaf forests," *Remote Sens. Environ.* **85(**4), 410-423 (2003) [doi: 10.1016/S0034-4257(03)00017-8].

[50] M. McCulloch, S. Fallon, T. Wyndham, E. Hendy, J. Lough, and D. Barnes, "Coral record of increased sediment flux to the inner Great Barrier Reef since European settlement," *Nature* **Vol. 421**, 727-730 (2003) [doi: 10.1038/nature01361].

[51] R. Bartley, M. Hartcher, A. Henderson, Y. Chen, and J. Brodie, "Application of the SedNet Model to the Bowen Catchment, Queensland: assessment of sediment and nutrient loads at a sub-catchment scale under different grazing scenarios. A Report to the Burdekin Dry Tropics Board for the NAP PAP 4 Project in the Bowen Catchment," Burdekin Dry Tropics Board and CSIRO, Canberra, (2004).

[52] I. P. Prosser, C. Moran, H. Lu, A. Scott, P. Rustomji, J. Stevenson, G. Priestley, C. H. Roth, and D. Post, "Regional Patterns of Erosion and Sediment Transport in the Burdekin River Catchment," CSIRO Land & Water, (2002).

[53] M. F. Hutchinson, J. L. Stein, and J. A. Stein, "Derivation of nested catchments and sub-catchments for the Australian continent," Canberra, Australia, (2000).

[54] C. H. Roth, G. Lawson, and D. Cavanagh, "Overview of key Natural Resource Management Issues in the Burdekin Catchment, with particular reference to Water Quality," CSIRO Land and Water Townsville, QLD, Australia, pp. 98 (2002).

[55] M. C. Hansen, R. S. Defries, J. R. G. Townshend, and R. Sohlberg, "Global land cover classification at 1 km spatial resolution using a classification tree approach," *Int. J. Remote Sens.* **21(**6), 1331 - 1364 (2000) [doi: 10.1080/014311600210209].

[56] R. B. Myneni, R. R. Nemani, and S. W. Running, "Estimation of global leaf area index and absorbed PAR using radiative transfer model," *IEEE Trans. Geosci. Remote Sens.* **35**, 1380-1393 (1997) [doi: 10.1109/36.649788].

[57] NASA, "MODIS Products Table," Land Processes Distributed Archive Center, last updated: 18 March 2009, https://lpdaac.usgs.gov/lpdaac/products/modis_products_table, (accessed: 22/4/2006).

[58] E. King, "LP DAAC MOD15A2 processing by CSIRO Marine and Atmospheric Research," Canberra, 2005.

[59] R. Myneni, S. W. Running, J. Glassy, and P. Votava, "User's Guide FPAR, LAI (ESDT: MOD15A2) 8-day Composite NASA MODIS Land Algorithm ", 1-17 (2003).

[60] B. Tan, J. N. Hu, D. Huang, W. Z. Yang, P. Zhang, N. V. Shabanov, Y. Knyazikhin, R. R. Nemani, and R. B. Myneni, "Assessment of the broadleaf crops leaf area index product from the Terra MODIS instrument," *Agric. For. Meteorol.* **135(**1), 124-134 (2005) [doi: 10.1016/j.agrformet.2005.10.008].

[61] M. Cuevas-Gonzalez, F. Gerard, H. Balzter, and D. Riano, "Studying the change in fAPAR after forest fires in Siberia using MODIS," *Int. J. Remote Sens.* **29**, 6873-6892 (2008) [doi: 10.1080/01431160802238427].

[62] J. Milne, "Evaluation of MODIS for groundcover and biomass/feed availability estimates in tropical savannah systems," Meat & Livestock Australia, Locked Bag 991, North Syndey, NSW, Australia, (2007).

[63] Department of the Environment and Water Resources, "Australia - Present Major Vegetation Groups - NVIS Stage 1, Version 3.0 (Albers 100m analysis product)," NVIS products for use at a national scale, last updated: 27 January 2010, http://www.environment.gov.au/metadataexplorer/explorer.jsp?goTo=details&docId=%7BF2C07BE8-0518-4232-9153-D4133E2E22A0%7D, (accessed: 6/4/2008).

[64] Department of the Environment and Water Resources, "Australia's Native Vegetation: A summary of Australia's Major Vegetation Groups," Canberra, ACT, (2007).

[65] R. J. Fensham, "Leichardt's maps: 100 years of change in vegetation structure in inland Queensland," *J. Biogeogr.* **35**, 141-156 (2008) [doi: 10.1111/j.1365-2699.2007.01777.x].

[66] R. Fensholt, "Earth observation of vegetation status in the Sahelian and Sudanian West Africa: comparison of Terra MODIS and NOAA AVHRR satellite data," *Int. J. Remote Sens.* **25(**9), 1641-1659 (2004) [doi: 10.1080/01431160310001598999].

[67] Y. Yi, D. Yang, J. Huang, and D. Chen, "Evaluation of MODIS surface reflectance products for wheat leaf area index (LAI) retrieval," *ISPRS J. Photogramm. Remote Sens.* **63(**6), 661-677 (2008) [doi: 10.1016/j.isprsjprs.2008.04.004].

[68] D. C. Steinberg and S. Goetz, "Assessment and extension of the MODIS FPAR products in temperate forests of the eastern United States," *Int. J. Remote Sens.* **30(**1), 169 - 187 (2009) [doi: 10.1080/01431160802244276].

[69] R. Fensholt, I. Sandholt, M. S. Rasmussen, S. Stisen, and A. Diouf, "Evaluation of satellite based primary production modelling in the semi-arid Sahel," *Remote Sens. Environ.* **105(**3), 173-188 (2006) [doi: 10.1016/j.rse.2006.06.011].

[70] K. F. Huemmrich and S. N. Goward, "Vegetation Canopy PAR Absorptance and NDVI: An Assessment for Ten Tree Species with the SAIL Model," *Remote Sens. Environ.* **61(**2), 254-269 (1997) [doi: 10.1016/S0034-4257(00)00184-X].

[71] R. B. Myneni, S. Hoffman, Y. Knyazikhin, J. L. Privette, J. Glassy, Y. Tian, Y. Wang, X. Song, Y. Zhang, and G. R. Smith, "Global products of vegetation leaf area and fraction absorbed PAR from year one of MODIS data," *Remote Sens. Environ.* **83(**1-2), 214-231 (2002) [doi: 10.1016/S0034-4257(02)00074-3].

[72] N. V. Shabanov, D. Huang, Y. Knjazikhin, R. E. Dickinson, and R. B. Myneni, "Stochastic radiative transfer model for mixture of discontinuous vegetation canopies," *J. Quant. Spectrosc. Radiat. Transfer* **107(**2), 236-262 (2007) [doi: 10.1016/j.jqsrt.2007.01.053].

[73] R. Bartley, C. H. Roth, J. Ludwig, D. McJannet, A. Liedloff, J. Corfield, A. Hawdon, and B. Abbott, "Runoff and erosion from Australia's tropical semi-arid rangelands: influence of ground cover for differing space and time scales," *Hydrol. Processes* **20(**15), 3317-3333 (2006) [doi: 10.1002/hyp.6334].

[74] Q. Zhang, X. Xiao, B. Braswell, E. Linder, F. Baret, and B. Moore, "Estimating light absorption by chlorophyll, leaf and canopy in a deciduous broadleaf forest using MODIS data and a radiative transfer model," *Remote Sens. Environ.* **99(**3), 357-371 (2005) [doi: 10.1016/j.rse.2005.09.009].

[75] P. Olofsson, L. Eklundh, F. Lagergren, P. Jönsson, and A. Lindroth, "Estimating net primary production for Scandinavian forests using data from Terra/MODIS," *Adv. Space Res.* **39(**1), 125-130 (2007) [doi: 10.1016/j.asr.2006.02.031].

[76] D. J. Barrett, M. J. Hill, L. B. Hutley, J. Beringer, J. H. Xu, G. D. Cook, J. O. Carter, and R. J. Williams, "Prospects for improving savanna biophysical models by using multiple-constraints model-data assimilation methods," *Austral. J. Bot.* **53(**7), 689-714 (2005) [doi: 10.1071/BT04139].